JOURNAL OF Materials CHEMISTRY

A computational investigation of the structure of κ-alumina using interatomic potentials

Gianluca Paglia,[a] Andrew L. Rohl,[b] Craig E. Buckley[a] and Julian D. Gale[c]

[a]*Department of Applied Physics, Curtin University of Technology, PO Box U1987, Perth 6845, Australia. Tel: +618 9266 3824; Fax: +618 9266 7192; E-mail: paglia@power.curtin.edu.au*
[b]*A.J. Parker C.R.C. for Hydrometallurgy, Department of Applied Chemistry, Curtin University of Technology, PO Box U1987, Perth 6845, Australia. Tel: +618 9266 3717; Fax: +618 9266 2300; E-mail: andrew@power.curtin.edu.au*
[c]*Department of Chemistry, Imperial College of Science, Technology and Medicine, South Kensington, UK SW7 2AY. Tel: +44 20 7594 5757; Fax: +44 20 7594 5804; E-mail: j.gale@ic.ac.uk*

Received 28th June 2001, Accepted 25th September 2001
First published as an Advance Article on the web 26th October 2001

The high industrial and technological importance of alumina warrants thorough investigation of its structure and properties. Although the stable α-alumina phase is well characterised, many of its metastable structures are not. One of these metastable structures, κ-alumina (κ-Al_2O_3), has been subject of a recent investigation using first principles calculations based on periodic density functional theory (DFT). The purpose of this paper is to investigate the structure of κ-Al_2O_3 using empirical modelling methods. A dipolar shell model is used to calculate the total energy, incorporating the Buckingham model for short-range repulsion and the Ewald method for electrostatic contributions. Four different sets of potential parameters are used for comparison. The resultant minimum energy configurations determined for three of the potential parameters used are found to be in agreement with each other, the first principles study, and experimental data.

Introduction

Because of its hardness, abrasion resistance, mechanical strength, corrosion resistance, and good electrical insulation, alumina (Al_2O_3) is a material of considerable technological and industrial significance.[1,2] It exists in a variety of metastable structures including the γ, η, θ, κ, and χ aluminas, as well as its stable α-alumina phase.[3,4] The phase transformations that occur during the calcination of the hydrated alumina phase, gibbsite ($Al(OH)_3$), to α-alumina (α-Al_2O_3) are of fundamental importance in designing ceramic processing procedures, which use partially-calcined starting material. The nature of these phase transformations has been studied for many years,[5] yet there still exists considerable controversy over the definitive structures of many of the Al_2O_3 phases. Without adequate knowledge of the structural form, research into the properties, dynamics and applications of these materials will always be less than optimal.

Unlike the α-Al_2O_3 phase, whose structure has been accurately known for a long time, only a few experimental studies have been performed on κ-alumina (κ-Al_2O_3).[6–11] This phase finds use in wear-resistant coatings in cutting-tool materials. However, difficulty in obtaining significant amounts of pure sample and the poor degree of crystallinity have hampered the experimental determination of its structure. Although the oxygen sublattice is well known from these studies, the uncertainty arises in the atomic positioning within the aluminium sublattice.

Only recently have confident claims as to the definitive κ-Al_2O_3 structure been made.[11–14] A study by Ollivier *et al.*,[11] based on X-ray diffraction (XRD), transmission electron microscopy (TEM) and nuclear magnetic resonance (NMR), concluded that the aluminium ions to be inserted between the oxygen layers in both octahedral and tetrahedral positions are in a 3 : 1 ratio. The study, by Yourdshahyan *et al.*,[12–14] employed first principles calculations based on periodic density functional theory (DFT), with a plane wave basis set. This was the first study to attempt to look at several possible structures for κ-Al_2O_3 instead of just pointing towards a specific structure. The final structure determined by Yourdshahyan *et al.*[14] for κ-Al_2O_3 exhibited lattice parameters differing by no more than ±0.1 Å from those determined by Ollivier *et al.*, and also found the aluminium ions to be octahedrally and tetrahedrally coordinated between the oxygen layers in a 3 : 1 ratio.

The purpose of this paper is to investigate the structure of κ-Al_2O_3 using empirical modelling methods and compare our results to those from the Yourdshahyan *et al.* study. Although modelling techniques based on interatomic potentials cannot yield accurate data with regards to electronic properties of materials, it is expected that they can produce reasonably accurate structural data in a fraction of the time taken by quantum mechanical calculations. *Ab initio* calculations on complex structures like κ-Al_2O_3 can take many days or weeks whereas the empirical modelling methods typically only involve a few seconds of computation time. This allows for an extensive search of all possible structural candidates to be performed rather than an "educated guess" at a restricted number of structural candidates.

Methodology

Structure

Recent transmission electron microscopy (TEM) and X-ray diffraction (XRD) studies have shown κ-Al_2O_3 to belong to the space group $Pna2_1$ and the orthorhombic crystal system with the *mm*2 point group.[6,8,9] Based on these experimental observations, the unit cell can be considered to be comprised

 DOI: 10.1039/b105664f

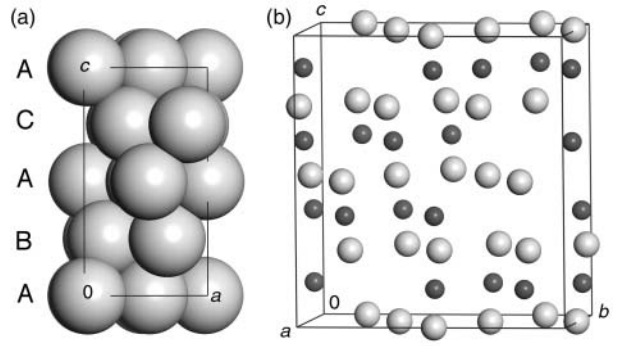

Fig. 1 (a) Illustration of the stacking sequence of the oxygen sublattice. (b) Idealised example of unit cell.

of 40 atoms in total, 24 oxygen atoms and 16 aluminium atoms. There are four layers in the oxygen sublattice, each comprising six oxygen atoms, exhibiting a close-packed ABAC... stacking sequence along the *c*-axis of the unit cell. Due to the stoichiometry of κ-Al_2O_3, the aluminium sublattice has four layers with four atoms, lying interstitially between the oxygen layers. This structural configuration is illustrated in Fig. 1. The Al atoms are capable of occupying octahedral and/or tetrahedral site positions.

The four symmetry related positions in the unit cell which arise due to the $Pna2_1$ symmetry are as follows: (x, y, z), $(\frac{1}{2}+x, \frac{1}{2}-y, z)$, $(\bar{x}, \bar{y}, \frac{1}{2}+z)$, and $(\frac{1}{2}-x, \frac{1}{2}+y, \frac{1}{2}+z)$. For κ-$Al_2O_3$ this means that the unit cell can be described using 10 independent atomic positions. For every independent starting coordinate a second is generated within the same plane and a second pair is located two planes below, *i.e.* in the $n+2$ plane.

The room temperature lattice parameters of the κ-Al_2O_3 unit cell have been determined to be $a=4.8351$ Å, $b=8.3109$ Å, and $c=8.9363$ Å by Halvarsson *et al.*[8] using XRD. Using convergent-beam electron diffraction with a TEM these parameters were determined to be $a=4.8437$ Å, $b=8.3300$ Å, and $c=8.9547$ Å by Liu and Skogsmo.[6]

Structure notation and candidates

In order to distinguish between alternative possible configurations of structure, a system of notation is required. In this examination of κ-Al_2O_3, a structure notation scheme identical to that of the Yourdshahyan *et al.* study is used, where the oxygen and aluminium positions are described by the type of stacking. Because the oxygen sublattice is well known[6,8,9] it can be fixed in one position while the possible configurations are considered for the interstitial Al ions. Each structure candidate is labelled with notation of the type $Aa_\alpha c_\gamma Bc_\alpha c_\gamma$; the stacking and pair types of the first two oxygen and aluminium layers (layers n and $n+1$) in the unit cell, allowing each possible unit cell to be implicitly described. This is achieved as a consequence of the symmetry, which allows the structure to be described using 10 independent atomic positions as the starting coordinates for the symmetry operators.

A, B (and C) in the $Aa_\alpha c_\gamma Bc_\alpha c_\gamma$-type notation represent the layers of oxygen ions in accordance with the ABAC··· stacking sequence. The lower case letters, a, b, and c, and their associated subscripts, α, β, and γ, represent Al pair positions within the layer, as shown in Fig. 2, where the ideal positions for each pair between the A and B layers are illustrated. The $a_\alpha c_\gamma$ configuration representing the 2 Al pairs in the layer n is generated by applying the first two symmetry operators of the $Pna2_1$ space group. Applying the remaining two symmetry operators yields $a_\alpha b_\beta$ in the $n+2$ layer. Similarly, the $c_\alpha c_\gamma$ configuration in the $n+1$ layer leads to $b_\alpha b_\beta$ pairs in the $n+3$ layer. Hence the $Aa_\alpha c_\gamma Bc_\alpha c_\gamma$-type notation can be extended to $Aa_\alpha c_\gamma Bc_\alpha c_\gamma Aa_\alpha b_\beta Cb_\alpha b_\beta$ in order to explicitly describe the unit cell.

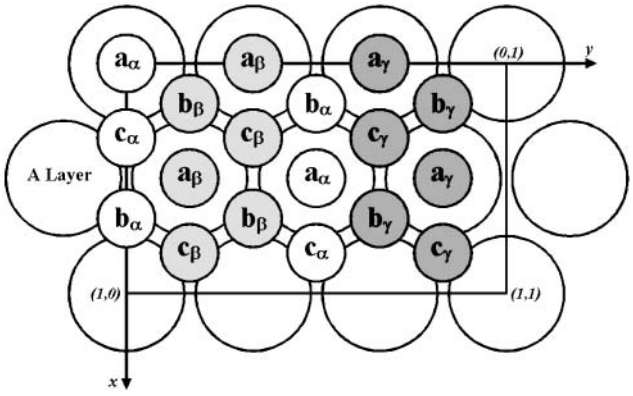

Fig. 2 Illustration of aluminium pair positions (labelled circles) between the A and B stacking layers of oxygen. After Yourdshahyan *et al.*[14]

The computational speed of the interatomic potentials used[15] allows for a more rigorous investigation of the structural candidates than the Yourdshahyan *et al.* study. Yourdshahyan *et al.* excluded structural candidates where Al pairs would be in adjacent sites on account of their presumed unfavourable energy. This left a total of 225 structure candidates which was then reduced to 60 after symmetry considerations. Such measures are necessary when using quantum mechanical techniques due to the computational expense.[16] In this study, the approach taken was to make no assumptions as to the likelihood of any configuration and to thus do an exhaustive search of all possible configurations.

On each independent layer there are 36 possible configurations for the two Al pairs. This gives rise to $36^2=1296$ different structures, after considering all possible combinations of the Al pairs between the two independent layers. This was reduced to 666 independent structural candidates after considering the artefact introduced by the structure notation; *i.e.* 630 of the 1296 candidates were doubled up as a consequence of the notation system as noted by Yourdshahyan *et al.* These degenerate structures were related through symmetry, *via* a 180° rotation of the unit cell around [010] and the translation $(\frac{1}{2}+x, \frac{1}{2}+y, z)$.[12]

Remaining consistent with the nomenclature used by Yourdshahyan *et al.*, the aluminium layers can be categorised in accordance with their Al pair coordination. *O* reflects all Al ions being situated in octahedral sites, *T* indicates complete tetrahedral site occupancy, and *M* (mixed) represents one pair in the octahedral and the other pair in tetrahedral positions. This allows independent structural possibilities to be grouped in six ways: *OO*, *OT*, *MO*, *MM*, *MT*, and *TT*, depending on the type of coordination in the first two layers.

In generating the 666 independent structural candidates, the oxygen sublattice was fixed at the same idealised positions for each possible structure, starting with the A stacking layer at the origin of the unit cell. Each subsequent stacking layer was positioned a fractional distance of 1/4 apart parallel to the *c*-axis of the unit cell. A program was used to generate the 666 possible independent configurations of the Al ions that were subsequently incorporated within the O sublattice, in accordance with the structure notation hitherto discussed, to complete each idealised unit cell. The *z*-axis positioning of the octahedrally and tetrahedrally coordinated Al ions was half and a quarter of the separation distance between the oxygen layers respectively. These 666 idealised independent candidates were then used as the starting configurations in the calculations. The same initial lattice parameters were used in this study as per the Yourdshahyan *et al.* study. These were (after extrapolation to 0 K by Yourdshahyan *et al.*, in Angstroms): $a=4.8041$, $b=8.2543$, and $c=8.8785$.

Table 1 Potentials parameters used in this study. Note: e = charge of an electron (1.602×10^{-19} C)

Authors		A/eV	ρ/Å	C/eV Å^{-6}	Truncation/Å	q(core)/e	q(shell)/e	k/eV Å^{-2}
Bush *et al.*[17]	Al^{3+}– O^{2-}	2409.505	0.2649	0.0	15.0	0.043	2.957	403.98
	O^{2-}– O^{2-}	25.41	0.6937	32.32	15.0	0.513	−2.513	20.53
Catlow *et al.*[18]	Al^{3+}– O^{2-}	1460.3	0.29912	0.0	10.0	3.000	—	—
	O^{2-}– O^{2-}	22764.0	0.14900	27.8790	12.0	0.86902	−2.86902	74.92
Minervini *et al.*[19]	Al^{3+}– O^{2-}	1725.20	0.28971	0.0	20.0	3.000	—	—
	O^{2-}– O^{2-}	9547.96	0.2192	32.0	20.0	0.04	−2.04	6.30
Mackrodt and Stewart[20]	Al^{3+}– O^{2-}	Cubic spline used (Ref. 20)				3.000	—	—
	O^{2-}– O^{2-}					−0.0260	−1.974	16.00

Computational details

Four different potential models applicable to aluminium oxides, all based on the Born ionic model, were employed (Table 1), namely those of Bush *et al.*, Catlow *et al.*, Minervini *et al.* and Mackrodt and Stewart.[17–20] All models consisted of short-range repulsive interactions, longer range attractive interactions, long range Coulombic interactions and atomic polarization. The first two types of interaction, describing the repulsion between atoms at short distances and the van der Waals attraction at longer distances, utilised a Buckingham potential in three of the four models

$$\varphi_{ij}(r) = A_{ij}\mathrm{e}^{-\left(\frac{r_{ij}}{\rho_{ij}}\right)} - \frac{C_{ij}}{r_{ij}^6} \quad (1)$$

where r_{ij} represents the separation distance between ions i and j, A_{ij} and ρ_{ij} are parameters describing the repulsion term and C_{ij} is the dispersion coefficient describing van der Waals attraction. The Mackrodt and Stewart model used electron gas methods to describe the short range interactions, using a cubic spline to interpolate the value of the potential. The long range electrostatic energy for all models was evaluated using the Ewald method.[21,22] Atomic polarisation was incorporated *via* the core–shell model where a massless shell is coupled to a core by a harmonic force[23]

$$E_{(\mathrm{core-shell})} = \frac{1}{2}kr^2 \quad (2)$$

where the shell and the core are Coulombically screened from each other. It should be noted that only the Bush *et al.* model employed the shell model for both aluminium and oxygen ions, while the other three assumed that the aluminium ion is not polarisable.

Constant volume simulations were performed using the rational function optimisation (RFO)[24] algorithm for minimisation of the total energy to ensure that the final hessian is positive definite. These minimisations were performed within the constraints of the space group symmetry to which κ-Al_2O_3 has been experimentally determined to belong.[6,8,9] The computational package employed for these calculations was the General Utility Lattice Program (GULP).[15,25] Constant pressure minimisations were performed on the lowest energy structures determined by the constant volume minimisations.

Discussion

For all potential sets used, every minimised structure is found to be considerably lower in energy than the starting configuration indicating that the coordinates strongly deviated from being idealised. The starting and minimised energies of all the 666 configurations calculated using the Bush *et al.* parameters are illustrated in Fig. 3 as an example. On this scale, the minimised configurations appear to have very similar energies. The lower energies of the starting structures towards the bottom right of Fig. 3 are due to the higher separation distances between Al pairs, both within and between layers. Often the minimised structural configurations were different from the starting configuration from which they were derived. For example, structure number 662 exhibits an $Ac_\alpha c_\gamma Bc_\alpha c_\beta$ starting configuration (*OO*-type coordination). However, after minimisation its configuration was $Ac_\alpha c_\beta Bb_\beta c_\gamma$ (*MO*-type coordination) for all sets of potentials used. Focussing in on the minimised energies (Fig. 4) shows that most starting

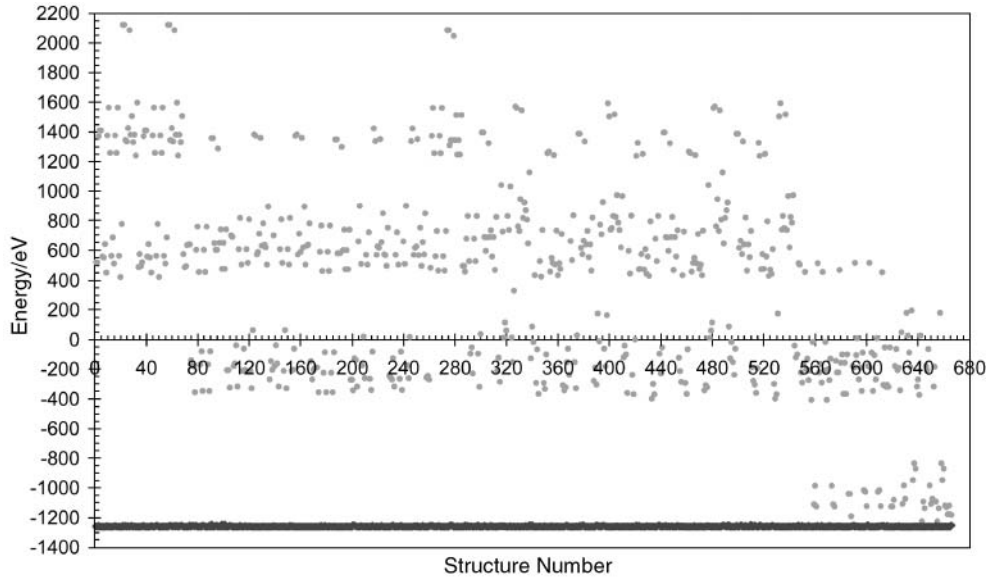

Fig. 3 Starting and minimised energies using the potentials of Bush *et al.*;[17] grey points = starting structure energy, black points = minimised structure energy.

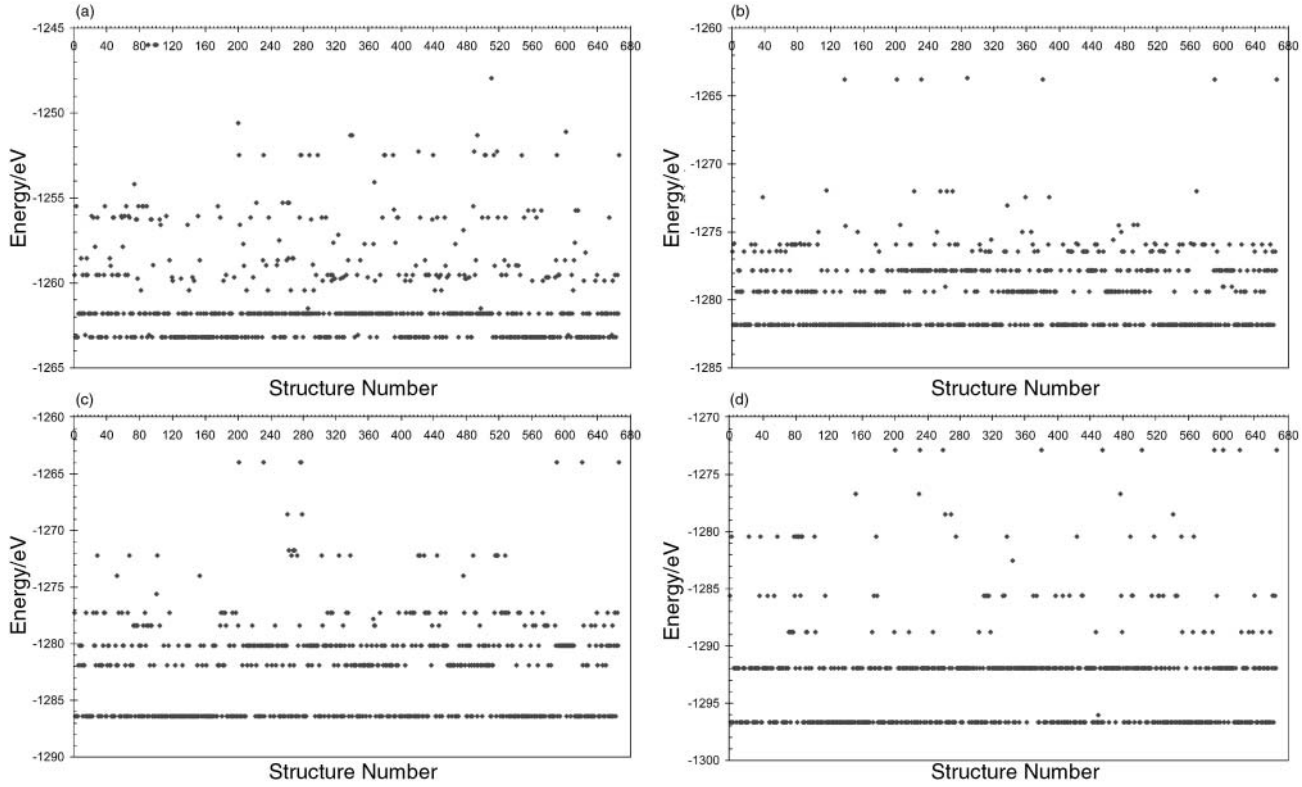

Fig. 4 Minimised energies achieved for each of the potentials incorporated into the Buckingham model: (a) Bush *et al.*,[17] (b) Catlow *et al.*,[18] (c) Minervini *et al.*,[19] (d) Mackrodt and Stewart.[20]

configurations minimise to one of only seven local minima. This behaviour is observed for all of the potential sets used, except for the Bush *et al.* potential set where there were ten common local minima. Each minimised energy value represents the same optimised structural configuration. This was verified by examining the Γ-point phonon frequencies and structural configurations themselves. It was also observed that the majority of structure candidates minimised to one of the two lowest energy structures.

The starting configurations appeared to have little bearing on the minimised configurations achieved. All minimised structures tended towards either *OO*, *OT* or *MO* coordination. For these final structures, particularly *MO* and *OT*, the minimised configuration was obtained from starting structures of each type of coordination possibilities (*i.e.* *OO*, *OT*, *MO*, *MM*, *MT*, and *TT*).

The lowest energy structure for each of the four sets of potential parameters used all exhibited *MO* coordination, of identical structural configuration (Fig. 5). The oxygen sublattice was found to remain in close proximity to the idealised starting coordinates upon optimisation, although sometimes a translation of the sublattice, to varying degrees along any one of the three crystallographic axes, was found. The resulting configuration was determined to be $Ac_{\alpha}c_{\beta}Bb_{\beta}c_{\gamma}Ab_{\alpha}b_{\gamma}Cb_{\beta}c_{\gamma}$. Cases existed where the minimised configuration was determined to be $Ac_{\alpha}c_{\gamma}Bb_{\gamma}c_{\beta}Ab_{\alpha}b_{\beta}Cb_{\gamma}c_{\beta}$, which is identical to the previous configuration through a 2_1 screw axis. The absence of imaginary values in the Γ-point phonon frequencies calculated at the lowest energy configuration for each potential set, combined with a search for higher symmetry within the Materials Studio software package,[26] confirms that all potential sets predict that the space group is $Pna2_1$, in agreement with the experimental observations of Liu and Skogsmo, and Halvarsson, Langer and Vuorinen.[6,8,9]

Within the lowest energy structure, significant distortion was evident for the octahedrally coordinated Al ion within the *M* layer, which was accompanied by some perturbation of the immediately adjacent oxygen layers. To illustrate the degree of this distortion, the average Al–O bond length within the octahedra associated with the c_{β} aluminium pair of the *O* layers was typically 1.91 Å, with the bond lengths ranging from 1.90 to 1.97 Å. In contrast, the average Al–O bond length within the octahedra associated with the c_{γ} aluminium pair of the *M* layers was 1.96 Å. Here the range in bond lengths was 1.81 to 2.37 Å. In this instance, aside from the longest bond length, 2.37 Å, the remaining five bond lengths averaged 1.88 Å, with the longest of these being 1.96 Å. This indicates that the distortion of the *M* layer octahedra is due to one extreme bond length.

Within the oxygen sublattice, the slight distortion near the octahedrally coordinated Al ions of the *M* layer tended to be out-of-plane deviations in the *z*-direction. Aside from this slight

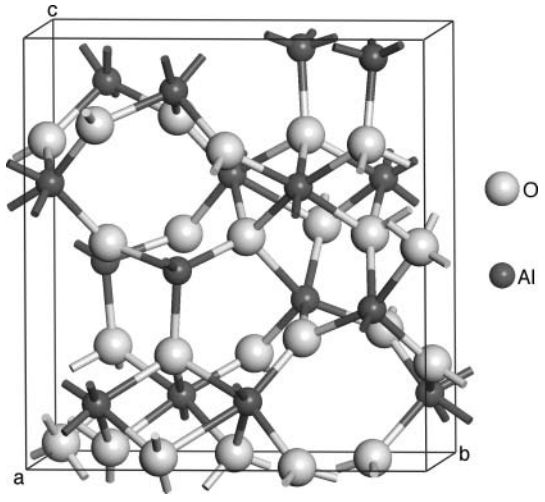

Fig. 5 Lowest energy structure from fixed cell parameter minimisations; *MO* coordination; atomic configuration: $Ac_{\alpha}c_{\beta}$ $Bb_{\beta}c_{\gamma}$ $Ab_{\alpha}b_{\gamma}$ $Cb_{\beta}c_{\gamma}$.

deviation, the oxygen sublattice remained close to the idealised starting configuration provided for the oxygen layers.

The rigidity of the oxygen sublattice was also evident in the highest energy minimised structure (in Fig. 4 this is the highest line of convergent energies) which exhibited *OO* coordination of the Al sublattice, the atom configuration being $Ac_{\beta}c_{\gamma}Bc_{\beta}$-$c_{\gamma}Ac_{\beta}c_{\gamma}Cc_{\beta}c_{\gamma}$. This was consistently found for all the four potential parameters sets. Compared to the lowest energy structure of *MO*-type coordination, there was very little distortion of the oxygen sublattice (there was no departure from the starting positions in the *z*-direction), which is attributable to the complete octahedral bonding of the Al ions. Furthermore, the nature of the eigenvalues suggests the $Ac_{\beta}c_{\gamma}Bc_{\beta}$-$c_{\gamma}Ac_{\beta}c_{\gamma}Cc_{\beta}c_{\gamma}$ structure is stable within the $Pna2_1$ space group symmetry.

All stable structures with total energies between the highest and lowest values exhibit *MO* or *OT* coordination, depending on the potential parameters used in the Buckingham model. For the Catlow *et al.* and Minervini *et al.* potential parameters these intermediate energy structures all exhibit *MO* coordination, while for the Bush *et al.* and Mackrodt and Stewart, the intermediates were all of *OT* coordination. There was a general trend of increased structural distortion for intermediate structures of higher total energy. In some cases the distortion was severe, to the extent where both ion species occupied the same plane.

The oxygen lattice of the intermediate structures, although appearing to exhibit the correct configuration, demonstrated a general trend of greater distortion with increasing structure energy. As with the lowest energy structure, this distortion tended to be out-of-plane. To illustrate the degree of this, a typical example of the out-of-plane movement of the oxygen sublattice, adjacent to the octahedrally coordinated c_{γ} Al pair of the *M* layer, was 0.445 Å. In the structure with the second lowest energy this was typically 0.651 Å. As the energy of the structure increased, such distortions were more widespread throughout the lattice. It was not uncommon to see over 1/3 of the oxygen sublattice significantly deviating from their starting coordinates for many of the intermediate structures, while the remainder of the lattice remained in place.

It is understandable that the observed distortions in the structure have occurred given the conditions under which the calculations were performed. The starting structures themselves were highly strained. Cell volumes were fixed with dimensions extrapolated to 0 K during optimisations in order to be consistent with the Yourdshahyan *et al.* study, whereas the potential parameters used were fitted for ambient temperature on the whole. However, the analysis has shown the lowest energy structure calculated here to be in good agreement with the lowest energy structure determined by Yourdshahyan *et al.*

Further optimisations were performed on the two most stable minimised structures and this time the lattice parameters were allowed to relax. For all potential sets, except those of Bush *et al.*, this did not change the nature of the lowest energy configuration, *i.e.* a *MO*-type structure with an $Ac_{\alpha}c_{\beta}Bb_{\beta}c_{\gamma}$-$Ab_{\alpha}b_{\gamma}Cb_{\beta}c_{\gamma}$ configuration.

It is at this stage that the Bush *et al.* potential parameters can be dismissed as unsuitable for the ionic crystal lattice calculations performed here. Although the Bush *et al.* potentials tended to yield the same trends, the results were not entirely consistent with those of the other three sets of potential parameters. This can be seen in Fig. 4 where there were 10 lines of convergent energies for Bush *et al.* (which were also more difficult to distinguish) as opposed to 7 for Catlow *et al.*, Minervini *et al.* and Mackrodt and Stewart. Furthermore, it can be seen from Fig. 4 that the results obtained using the Bush *et al.* parameters contained, by far, the greatest number of anomalous energies. Finally, although the structure obtained from the second set of optimisations met the conditions of convergence, it was highly distorted and bore no resemblance to the structure from which it was derived or those which resulted for the other three potential parameters used. The calculated structural data for the Catlow *et al.*, Minervini *et al.* and Mackrodt and Stewart sets of potential parameters can be found in Tables 2 and 3.

Assessment of the resulting stable structures (Fig. 6) for each set of potential parameters and comparison of the unit cell parameters (Table 2) has shown the Catlow *et al.* structure to be closest to that of the Yourdshahyan *et al.* study and

Table 2 Lattice parameters for the κ-Al_2O_3 structure

	Experimental		Simulated			
				This study		
	Liu and Skogsmo[6]	Halvarsson *et al.*[8]	Yourdshahyan *et al.*[14]	Catlow *et al.*[18]	Minervini *et al.*[19]	Mackrodt and Stewart[20]
a/Å	4.8437	4.8351	4.8041	4.8515	4.8473	4.8520
b/Å	8.3300	8.3109	8.2543	8.1693	8.2124	8.5425
c/Å	8.9547	8.9363	8.8785	8.8600	9.0119	9.1480
V/Å^3	361.3044	359.09	352.07	351.15	358.75	379.17

Table 3 Calculated atomic coordinates for the κ-Al_2O_3 structure

	Catlow *et al.*[18]			Minervini *et al.*[19]			Mackrodt and Stewart[20]		
Atom	*x*	*y*	*z*	*x*	*y*	*z*	*x*	*y*	*z*
O(1)	0.84921	0.84385	0.75000	0.85347	0.84153	0.75000	0.87041	0.83662	0.75000
O(2)	0.47939	0.51607	0.51923	0.48600	0.51316	0.51943	0.48434	0.50289	0.51312
O(3)	0.02964	0.66951	0.52790	0.02726	0.67039	0.52699	0.02912	0.67904	0.51979
O(4)	0.95439	0.67419	0.00521	0.95571	0.67696	0.00740	0.97941	0.67627	0.00206
O(5)	0.34573	0.33720	0.79380	0.35675	0.33361	0.78917	0.36144	0.32952	0.77583
O(6)	0.84839	0.48899	0.73256	0.85850	0.49354	0.73916	0.86305	0.49349	0.73316
Al(1)	0.31192	0.96009	0.15054	0.30724	0.95542	0.14998	0.31026	0.95014	0.14332
Al(2)	0.80819	0.16234	0.14468	0.80554	0.16041	0.14405	0.80120	0.15872	0.13688
Al(3)	0.20384	0.13933	0.44983	0.20727	0.13991	0.44503	0.18512	0.14887	0.43926
Al(4)	0.30361	0.64885	0.36646	0.29583	0.64743	0.36812	0.29174	0.64820	0.35832

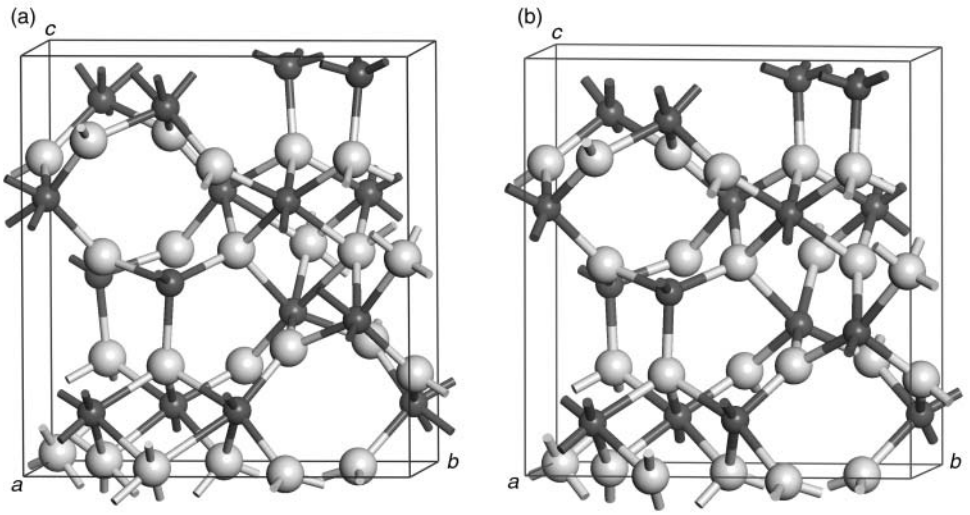

Fig. 6 (a) Lowest energy structure determined using the potential parameters of Catlow *et al.*;[18] (b) Lowest energy structure determined by Yourdshahyan *et al.*[14]

experiment.[6,8] All lattice parameters determined in this study were within 1.7% of the experimental values (Table 2), with the exception of two from the Mackrodt and Stewart stable structure which were within 2.8%. In particular the lattice parameters determined from the Catlow *et al.* parameters were within 1% of the experimental lattice parameters.[6,8] Considering the approximations made by interatomic potentials, this compares extremely well to first principles calculations, which were also found to be within 1% of the experimental lattice parameters.[6,8]

Yourdshahyan *et al.* determined the lowest energy structure for κ-Al_2O_3 to also have *MO*-type coordination, with an $Ac_\beta b_\gamma Bc_\alpha c_\gamma Ab_\gamma c_\beta Cb_\alpha b_\beta$ configuration. This structure is related to that determined in this study, by symmetry, through a 180° rotation about the [020] axis. These two resultant structures are compared in Fig. 6, where it is evident that quantum mechanical calculations make the lattice more rigid than the interatomic potentials. Yourdshahyan *et al.* also reported anisotropy in the structure, where there was closer packing of the aluminium ions in the [100] direction than in the [010], confirming thermal expansion measurements.[8] This anisotropy was also observed here.

The O–O bond distances ranged between 2.52–2.87 Å, 2.57–2.85 Å, and 2.67–2.94 Å, for the Catlow *et al.*, Minervini *et al.* and Mackrodt and Stewart optimised structures, respectively. These compare well with the range of 2.52–3.00 Å in the final structure determined by Yourdshahyan *et al.* and also agree with the empirical ionic radii of Pauling[27] and Shannon.[28] These latter authors indicate that an O–O bond length should be 2.8 Å, which lies within the range found here. Furthermore, Pauling has indicated that O–O bonds along edges shared by two polyhedra should be shorter, as was found to be the case here and in the work of Yourdshahyan *et al.*

In the case of the Al–O bond lengths within the octahedra of the stable structure, Yourdshahyan *et al.* reported these to vary between 1.79 and 2.20 Å, with the average within each octahedron ranging from 1.90 to 1.94 Å. The ranges in the Al–O bond lengths calculated here were 1.79–2.33 Å, 1.79–2.36 Å, and 1.79–2.39 Å for the stable structures determined using the Catlow *et al.*, Minervini *et al.* and Mackrodt and Stewart potential parameters, respectively. Also, average bond lengths for each octahedron varied from 1.90–1.94 Å, 1.89–1.96 Å, and 1.90–2.00 Å. These values were averaged over the whole unit cell. However, there are three pairs of octahedra within the two independent layers of the κ-Al_2O_3 structure, two in the *O* layer and one in the *M* layer, and in Table 4 the results are given separately. Further comparison can be found in the Al–O bond lengths, within octahedra, of Shannon, being between 1.895 and 1.925 Å.

Each of these pairs of octahedra was found to exhibit a different degree of distortion. It is therefore pertinent to examine the nature of the bonding and distortions more thoroughly (Table 4). To provide the appropriate comparison, the same expression was used to quantify the distortion as per Yourdshahyan *et al.*:

$$\Delta = \frac{1}{N}\sum_{i=1}^{N}\left(\frac{R_i - R_{av}}{R_{av}}\right)^2 \quad (3)$$

where N is the number of corners of the polyhedron, R_i is an

Table 4 Al–O bond length data within the octahedra of the κ-Al_2O_3 structure

				This study		
	Al pair (this study)		Yourdshahyan *et al.*[14]	Catlow *et al.*[18]	Minervini *et al.*[19]	Mackrodt and Stewart[20]
O Layer	c_α	Range/Å	1.79–2.19	1.79–2.17	1.79–2.23	1.79–2.24
		Average/Å	1.93	1.92	1.94	1.90
		Δ	51×10^{-4}	47×10^{-4}	72×10^{-4}	67×10^{-4}
	c_β	Range/Å	1.79–1.94	1.79–1.94	1.80–1.94	1.90–2.03
		Average/Å	1.90	1.90	1.89	1.94
		Δ	7.2×10^{-4}	6.9×10^{-4}	8.0×10^{-4}	12×10^{-4}
M Layer	c_γ	Range/Å	1.80–2.20	1.79–2.33	1.80–2.36	1.83–2.39
		Average/Å	1.94	1.94	1.96	2.00
		Δ	55×10^{-4}	90×10^{-4}	94×10^{-4}	95×10^{-4}

individual Al–O bond length, and R_{av} is the average Al–O bond length within the polyhedron.[27] The relative size of the distortions in each of the octahedra was found to agree with those of Yourdshahyan *et al.*

The Al–O distances within the tetrahedra of the stable structure ranged between 1.75–1.79 Å, 1.75–1.79 Å, and 1.74–1.79 Å for Catlow *et al.*, Minervini *et al.* and Mackrodt and Stewart, respectively, with averages of 1.78 Å, 1.78 Å, and 1.77 Å. The value reported by Yourdshahyan *et al.* was a range of 1.73–1.77 Å, and an average of 1.75 Å, for the Al–O lengths within the tetrahedra. Shannon provides Al–O values between 1.75 and 1.77 Å for tetrahedra. In light of these results, it is concluded that in this study the Al–O bond lengths calculated for both octahedra and tetrahedra agree with the results of Yourdshahyan *et al.* and the values provided by Shannon.

Further comparison of the structures determined here shows that they are in good agreement with that determined by Ollivier *et al.* who found the Al–O bonds within the octahedra to vary between 1.72 and 2.27 Å. The lattice parameters were determined by Ollivier *et al.* to be $a=4.8437$ Å, $b=8.3300$ Å and $c=8.9547$ Å. With the exception of the b lattice parameter of the Mackrodt and Stewart structure (which shows a 4.0% deviation) the largest difference between those of Ollivier *et al.* and the present work is 1.9%. with an average deviation of 0.9%. A direct comparison with the parameters of Yourdshahyan *et al.* and those determined here shows average deviations of 0.7, 0.8 and 1.9% for the potentials of Catlow *et al.*, Minervini *et al.* and Mackrodt and Stewart, respectively.

Conclusions

The purpose of this paper was to investigate the structure of κ-Al_2O_3, using interatomic potentials and compare the results with first principles calculations and experimental determinations. Of the four sets of potential parameters examined, only one, those of Bush *et al.*, proved unsuitable for this particular study. The remaining three were found to predict the same most stable structure, which in turn was in close agreement to the first principles calculations of Yourdshahyan *et al.* and experiment.[6,8,9,11] Furthermore, of these three sets of potential parameters, those of Catlow *et al.* were found to produce the results which most closely matched the first principles study.

It can therefore be concluded that the stable structure of κ-Al_2O_3 is of *MO*-type coordination, with $Ac_\alpha c_\beta Bb_\beta c_\gamma$-$Ab_\alpha b_\gamma Cb_\beta c_\gamma$ configuration. This is equivalent to $Ac_\beta b_\gamma Bc_\alpha$-$c_\gamma Ab_\gamma c_\beta Cb_\alpha b_\beta$, reported by Yourdshahyan *et al.* through symmetry.

Interatomic potentials have therefore proven suitable for use in such investigations where stable structures need to be determined from an enormous number of possibilities. In this case, the speed of interatomic potentials has enabled every possible starting configuration of κ-Al_2O_3 to be investigated, four times over, in a fraction of the time compared to the DFT study. Furthermore, the empirical method used also delivered an acceptable level of accuracy. With this in mind it makes sense to begin any computational study with a broad survey of possible outcomes, using faster methods, before striving to achieve high accuracy for a few cases.

Acknowledgements

This work originated from discussions with Yashar Yourdshahyan who provided valuable input and inspired a new direction in our research focus.

References

1 W. D. Kingery, H. K. Bowen and D. R. Uhlmann, *Introduction to Ceramics*, 2nd edn., John Wiley & Sons, New York, 1976.
2 C. N. Saterfield, *Heterogeneous Catlysis in Practice*, McGraw-Hill, New York, 1980.
3 H. C. Stumpf, A. S. Russell, J. W. Newsome and C. M. Tucker, *Ind. Eng. Chem.*, 1950, **48**, 1398.
4 B. C. Lippens and J. H. De Boer, *Acta Crystallogr.*, 1964, **17**, 1312.
5 R. S. Zhou and R. L. Snyder, *Acta Crystallogr., Sect. B*, 1991, **47**, 617.
6 P. Liu and J. Skogsmo, *Acta Crystallogr., Sect. B*, 1991, **47**, 425.
7 P. Hansson, M. Halvarsson and S. Vuorinen, *Surf. Coat. Technol.*, 1995, **76–77**, 256.
8 M. Halvarsson, V. Langer and S. Vuorinen, *Surf. Coat. Technol.*, 1995, **76–77**, 358.
9 M. Halvarsson, V. Langer and S. Vuorinen, *Powder Diffract.*, 1999, **14**, 61.
10 H.-L. Cross and W. Mader, *Chem. Commun.*, 1997, 55.
11 B. Ollivier, R. Retoux, P. Lacorre, D. Massiot and G. Ferey, *J. Mater. Chem.*, 1997, **7**, 1049.
12 Y. Yourdshahyan, C. Ruberto, L. Bengtsson and B. I. Lundqvist, *Phys. Rev. B: Condens. Matter*, 1997, **56**, 8553.
13 Y. Yourdshahyan, U. Engberg, L. Bengtsson, B. I. Lundqvist and B. Hammer, *Phys. Rev. B: Condens. Matter*, 1997, **56**, 8721.
14 Y. Yourdshahyan, C. Ruberto, M. Halvarsson, L. Bengtsson, V. Langer, B. I. Lundqvist, S. Ruppi and U. Rolander, *J. Am. Ceram. Soc.*, 1999, **82**, 1365.
15 J. D. Gale, *J. Chem. Soc., Faraday Trans.*, 1997, **93**, 629.
16 M. C. Payne, M. P. Teter, D. C. Allan, T. A. Arias and J. D. Joannopoulos, *Rev. Mod. Phys.*, 1992, **64**, 1045.
17 T. S. Bush, J. D. Gale, C. R. A. Catlow and P. D. Battle, *J. Mater. Chem.*, 1994, **4**, 831.
18 C. R. A. Catlow, R. James, W. C. Mackrodt and R. F. Stewart, *Phys. Rev. B: Condens. Matter*, 1982, **25**, 1006.
19 L. Minervini, M. O. Zacate and R. W. Grimes, *Solid State Ionics*, 1999, **116**, 339.
20 W. C. Mackrodt and R. F. Stewart, *J. Phys. C*, 1979, **12**, 431.
21 P. P. Ewald, *Ann. Phys.*, 1921, **64**, 253.
22 M. P. Tosi, *Solid State Phys.*, 1964, **16**, 1.
23 B. G. Dick and A. W. Overhauser, *Phys. Rev.*, 1958, **112**, 90.
24 A. Banerjee, N. Adams, J. Simons and R. Shepard, *J. Phys. Chem.*, 1985, **89**, 52.
25 J. D. Gale, *Philos. Mag. B*, 1996, **73**, 3.
26 Materials Studio version 1.2, Molecular Simulations Inc., San Diego, CA, 2001.
27 L. Pauling, *The Nature of the Chemical Bond*, 2nd edn., Cornell University, Ithaca, NY, 1944, pp. 396–400.
28 R. D. Shannon, *Acta Crystallogr., Sect. A*, 1976, **32**, 751.